7 SPACE-TIME TRELLIS CODED TRANSMIT DIVERSITY

In the foregoing chapters layered space-time coded transmit diversity techniques have been proposed to benefit from antenna diversity in the downlink, while putting the diversity burden on the BSS. Recall, the usefulness of the space-time processing hinges on the separation of the spatial and temporal signatures of the signal of interest. In [201, 202] space-time trellis coding has been introduced proposing joint design of coding, modulation, transmit diversity and optional receive diversity.

In line with the goals of this thesis, this chapter investigates the extension of the classical convolutional and turbo coded transmit diversity techniques to incorporate trellis (TCM) and turbo trellis coded modulation (TTCM). When higher modulation formats are considered for cellular CDMA, for instance changing from BPSK/QPSK to multi-dimensional modulation (e.g. multi-dimensional Q^2PSK [227, 228]), the use of TCM and TTCM techniques will be indispensable.

TCM has evolved over the past two decades as a combined coding and modulation technique for digital transmission over band-limited channels. The main advantage of TCM over classical coding schemes is the fact that trellis coding, and the resulting data-transmission strategy, does not expand the transmission bandwidth. It is both a power- and a bandwidth-efficient modulation scheme. TCM schemes use redundant non-binary modulation in combination with a finite-state encoder that determines the corresponding signal shape to be transmitted over the channel. At the receiver, the corrupted signals are decoded by a soft-decision ML Viterbi or MAP decoder. According to Ungerboeck [24, 189, 190] simple four-state TCM schemes can improve the robustness of digital transmission against additive noise by 3 *dB*, compared to conventional uncoded modulation. With more complex TCM schemes the coding gain can reach 6 *dB* or more.

As has been discussed in Chapter 4, the use of the Ungerboeck codes do yield a performance advantage over standard convolutional codes when combined in a RAKE-receiver CDMA system [44]. It is important to note that for single-user receivers, such as the MF or RAKE used in a multiuser environment, coding gain comes at the cost of increased MAI level. A limitation to the use of low rate coding comes when the spreading is reduced to such a level that the MAI does not appear no longer Gaussian. When transmit diversity signalling is considered, codes optimized for the AWGN channel may again be considered. By

using more powerful codes than those used by Boudreau *et al.* [44], the issue of trellis coded spreading can be more adequately addressed. Specifically, when space-time turbo coded modulation is considered, the potential coding gain can be substantial.

The focus is placed on the design and evaluation of diagonally layered space-time coded modulation (STCM) schemes for cellular CDMA. The space-time encoder selects the constellation symbols to transmit such that both diversity and coding gain are maximized. Towards this goal, three STCM schemes, namely orthogonal transmit diversity (OTD) [229, 230, 231], delay transmit diversity (DTD) [232], and the Alamouti code transmit diversity (ACTD) are considered for CDMA [151]. Both OTD and ACTD have been adopted by 3G CDMA systems in the U.S. and Europe, respectively.

Here, the performance of these diversity schemes is analyzed from a coding perspective in terms of product distance comparisons. Also, a heuristic approach based on classical multiple trellis-coded modulation (MTCM) techniques is adopted for the design of STCM codes.

7.1 SPACE-TIME TRELLIS CODED MODULATION SYSTEM MODEL

Figure 7.1 illustrates the components of a CDMA space-time trellis coded modulation system. The outer channel encoder receives a sequence of input symbols $\mathbf{b}$, and outputs a sequence of symbols

$$\mathbf{x} = \ldots, x_1, x_2, x_3, \ldots, x_n \,, \tag{7.1}$$

from the alphabet $\{0, 1, \ldots, M\}$, where M is the number of symbols available for transmission. The encoded symbols are then interleaved, using a block symbol-by-symbol interleaver. The function of the interleaver/de-interleaver is to distribute channel errors randomly throughout the decoder input sequence $\mathbf{y}$, thereby enabling the use of coding, optimal for AWGN, to function well under adverse MAI and multi-path fading. As shown in Figure 7.1, the interleaver outputs the symbol sequence, $\tilde{\mathbf{x}}$.

The sequence of channel encoder output symbols has a very carefully controlled structure that enables the detection and correction of transmission errors. The inner space-time code encoder should be designed in such a way that its combined spatial and temporal properties will guarantee maximum transmit diversity, while maintaining the option to include receive diversity. The (outer or first stage) channel coding may be either convolutional or turbo coding, or their trellis coded modulation variants.

After encoding, the output is split into M_T streams and each of the streams are independently spread by the same spreading sequence. The RF modulation and demodulation operations have been omitted. The code/time division transmit diversity system generates a signalling waveform based on the combinations of data modulation, spreading modulation, trellis coding and space-time encoded transmit diversity schemes.

Since the signal at the receive antenna is a linear superposition of the $K \times M_T$ transmitted orthogonal signals, the receiver first performs chip waveform matching with reference to the M_T streams associated with the desired user. This despreading operation is the key function of any spread-spectrum system, and can be accomplished only if accurate synchronization information is available. Here, perfect spreading waveform synchronization, carrier recovery, symbol and frame synchronization are assumed. Channel estimation is performed on each resolved path, and used in the pilot symbol assisted (PSA) RAKE combiner to resolve each of the transmitted streams from the multiple transmit antennas.

After down-convertion, de-spreading and RAKE combining, the symbol spaced receive samples are first decoded by the space-time decoder. Soft values are generated by the space-time decoder using a MAP or

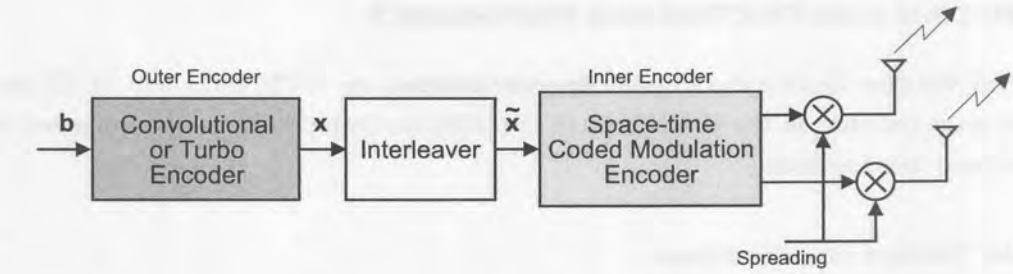

(a)

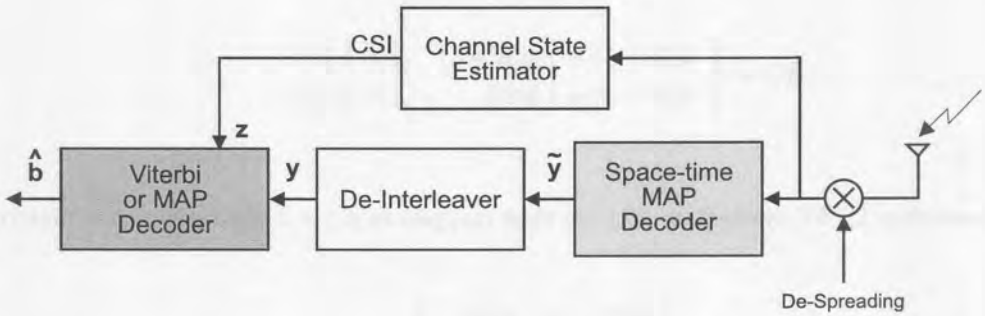

(b)

Figure 7.1. Block diagram of space-time coded transmit diversity system for CDMA.

the SOVA, and sent to the channel decoder for the outer decoding stage. To assist the channel decoder, additional reliability information can be obtained by measuring the CSI. The output of the CSI is denoted $\mathbf{z} = z_1, z_2, z_3, \ldots$ where z_j is a scaled real value.

The space-time diversity channel may be completely characterized by the probability that the channel output is $\mathbf{y}$, given that the channel input is $\mathbf{x}$ and $\mathbf{z}$ is the CSI. That is, the channel is completely characterized by

$$p(\mathbf{y} \mid \mathbf{x}, \mathbf{z}) = \prod_{i=1}^{\infty} p(y_i \mid x_i, z_i) \,, \tag{7.2}$$

where $p(y_i \mid x_i, z_i)$ is the probability that, given the input x_i and the CSI z_i, the demodulator output is y_i for channel i.

The probabilities $p(y_i \mid x_i, z_i)$ are found by analysis of the data modulation/demodulation, and the waveform channel, including transmit diversity. When the demodulator output is continuous, the probabilities of (7.2) are replaced by continuous probability density functions. Characterization of the channel using (7.2) enables decoupling of the analysis of the waveform channel from the FEC analysis.

The principle goal of the remainder of this chapter is to consider in detail the construction and performance evaluation of layered STCM codes for CDMA communication systems operating on frequency selective multiple access channels. This will be accomplished using the space-time coded system model described in this section. In the analysis perfect synchronization is assumed and it is further assumed that the MAI is Gaussian distributed (making use of the Gaussian assumption). In addition, perfect power control is assumed, implying that the base station adjusts the transmitted power such that the mobile terminal observes a prescribed SINR. Also, the analysis is restricted to QPSK ($M = 4$) modulation.

7.2 INNER CODE CONSTRUCTION AND PERFORMANCE

In this section, the three block coded transmit diversity schemes, viz. OTD, DTD, and ACTD are proposed for the first stage encoding in the STCM system. In [150], the latter schemes were proposed for TDMA based space-time coded systems.

7.2.1 Coded Transmit Diversity Schemes

7.2.1.1 Orthogonal Transmit Diversity (OTD). The channel coded bit sequence $b(i) = \pm 1$ is first mapped to QPSK symbol sequences $d(i)$, according to

$$d(i) = \begin{cases} b(2i-1) + j\, b(2i+1) & ,i = 1,3,5,\ldots \\ b(2i-2) + j\, b(2i) & ,i = 2,4,6,\ldots \end{cases}, \tag{7.3}$$

where $j = \sqrt{-1}$.

Every two consecutive QPSK symbols in $d(i)$ are then mapped to a 2×2 space-time code matrix

$$\mathbf{D}(i) = \begin{bmatrix} d(2i-1) & d(2i) \\ d(2i-2) & -d(2i) \end{bmatrix}, i = 1,2,\ldots \tag{7.4}$$

where the first column of $\mathbf{D}(i)$ is the temporal dimension and the second column is the spatial dimension.

The received samples corresponding to $\mathbf{D}(i)$ is given by

$$\begin{bmatrix} r(2i-1) \\ r(2i) \end{bmatrix} = \begin{bmatrix} d(2i-1) & d(2i) \\ b(2i-2) & -d(2i) \end{bmatrix} \cdot \begin{bmatrix} c_1 \\ c_2 \end{bmatrix} + \begin{bmatrix} \eta(2i-1) \\ \eta(2i) \end{bmatrix}, \tag{7.5}$$

where c_1 and c_2 are the independent diversity components and $\eta(2i-1)$ and $\eta(2i)$ are AWGN samples. Since the symbols are orthogonal across the antennas, the MAP decoder of an OTD code matrix simply calculates the statistics

$$\begin{aligned} \lambda(2i-1) &= c_1^* \left(r(2i-1) + r(2i)\right) \\ &= 2 \mid c_1 \mid^2 d(2i-1) + c_1^* \left(\eta(2i-1) + \eta(2i)\right), \\ \lambda(2i) &= c_2^* \left(r(2i-1) - r(2i)\right) \\ &= 2 \mid c_2 \mid^2 d(2i) + c_2^* \left(\eta(2i-1) - \eta(2i)\right), \end{aligned} \tag{7.6}$$

corresponding to $d(2i-1)$ and $d(2i)$, from $r(2i-1)$ and $r(2i)$, respectively, and determines to which quadrant in the QPSK constellation the symbols most likely belong. The likelihood (or confidence level) of this determination is the soft output passed on to the channel decoder.

Essentially, OTD sends half of the coded bits from one antenna and the other half of the coded bits from the other antenna. The diversity is achieved at the channel coding level since half of the coded bits fade independently from the other half. The space-time mapping does not provide any diversity advantage.

The OTD scheme is not restricted to two antennas. In general, any $M_T \times M_T$ unitary transformation can map M_T symbols into an $M_T \times M_T$ orthogonal code matrix.

7.2.1.2 Delay Transmit Diversity (DTD). In delay transmit diversity (DTD) the BSS transmit a delayed version of the original signal [232]. It was shown in [229] that DTD has a limited link performance gain over non-transmit diversity due to its adverse effect of degrading orthogonality and increasing the interference level at the mobile receiver.

In the DTD scheme, the first antenna sends the original QPSK sequence in (7.3) while the second antenna sends the sequence with one symbol delay. This artificially creates a dispersive channel with two equal-strength symbol-spaced channel components. As in OTD, DTD can be extended to any number of antennas with different transmit diversity delays.

7.2.1.3 Alamouti Code Transmit Diversity (ACTD). The paper by Alamouti [151], revealed a very simple yet effective block code of length 2 for a two antenna system. It maps two symbols into a 2×2 code matrix according to

$$\mathbf{D}(i) = \begin{bmatrix} d(2i-1) & d(2i) \\ -d^*(2i) & d^*(2i-1) \end{bmatrix}, i = 1, 2, \ldots . \tag{7.7}$$

Since the symbols are also orthogonal across antennas, the soft-input trellis decoder simply calculates

$$\begin{aligned} \lambda(2i-1) &= c_1^* \ (r(2i-1) + c_2 \, r^*(2i)) \\ &= \left(|\, c_1 \,|^2 + |\, c_2 \,|^2\right) d(2i-1) + c_1^* \, \eta(2i-1) + c_2 \, \eta^*(2i) \, , \\ \lambda(2i) &= c_2^* \ (r(2i-1) - c_1 \, r^*(2i)) \\ &= \left(|\, c_1 \,|^2 + |\, c_2 \,|^2\right) d(2i) + c_2^* \, \eta(2i-1) - c_1 \, \eta^*(2i) \, . \end{aligned} \tag{7.8}$$

7.2.2 *Inner Code Performance Considerations*

In an attempt to simplify the analysis, it is assumed that the channels in consideration are stationary and flat. These assumptions correspond to the condition where transmit diversity is most effective, i.e., the condition in which the terminal is moving very slowly in a single path fading environment. An indoor environment is well approximated by this model. Furthermore, it is assumed that the conditions of fading are independent (uncorrelated) across antennas.

Under conditions of the foregoing channel assumptions and assuming that the propagation delays are the same for all antennas, the received symbol-spaced samples of a transmitted "code matrix" $\mathbf{D}$ are defined as

$$\mathbf{D}(i) = \begin{bmatrix} d_1(1) & d_2(1) & \ldots & d_{M_T}(1) \\ d_1(2) & d_2(2) & \ldots & d_{M_T}(2) \\ \vdots & \vdots & . & \vdots \\ d_1(n) & d_2(n) & \ldots & d_{M_T}(n) \end{bmatrix} , \tag{7.9}$$

where $d_l(n)$, denoting the symbol transmitted by the lth antenna at time n, can be expressed in a matrix form as

$$\begin{aligned} r(1) &= \sum_{l=1}^{M_T} d_l(1)\, c_l \;+\; \eta(1)\,, \\ r(2) &= \sum_{l=1}^{M_T} d_l(2)\, c_l \;+\; \eta(2)\,, \\ &\vdots \\ r(n) &= \sum_{l=1}^{M_T} d_l(n)\, c_l \;+\; \eta(n)\,, \end{aligned} \tag{7.10}$$

where c_l denotes the i.i.d. zero-mean complex Gaussian channel component of the lth antenna, $\eta(n)$ denotes the i.i.d. AWGN at the nth symbol time, and $d_l(n)$ is the symbol transmitted by the lth antenna at the nth symbol time.

The pairwise error probability, $P_d(\mathbf{D} \to \hat{\mathbf{D}})$ of decoding a code matrix $\hat{\mathbf{D}}$, into $\mathbf{D}$ was derived in [149]. It was shown that the distance between the two code matrices is determined by the eigenvalues of $(\hat{\mathbf{D}}-\mathbf{D})^H(\hat{\mathbf{D}}-\mathbf{D})$ and that in order to achieve full diversity, the difference between any pair of code matrices must have full rank. Approximations given in [201, 202] lead to the definition of the product distance E_P [233], between two code matrices $\hat{\mathbf{D}}$, and $\mathbf{D}$ as

$$E_P = \left|(\hat{\mathbf{D}} - \mathbf{D})^H(\hat{\mathbf{D}} - \mathbf{D})\right| . \tag{7.11}$$

With (7.11), the distance properties of the three coded diversity schemes under investigation are compared. Since the channels are stationary, the interleaver is not taken into account in the inner code analysis presented here.

Making extensive use of the analysis carried out by Guey [150], the coded diversity schemes performance is considered. The product distances for OTD, DTD, ACTD, considering the difference between two distinct information sequences $\mathbf{X}$ and $\mathbf{Y}$ differing in P symbol intervals, are given by

$$E_{P_{OTD}}(\mathbf{X},\mathbf{Y}) = 4\left(\sum_{i=1}^{P/2} |\,\delta(2i-1)\,|^2\right)\cdot\left(\sum_{i=1}^{P/2} |\,\delta(2i)\,|^2\right), \tag{7.12}$$

$$E_{P_{DTD}}(\mathbf{X},\mathbf{Y}) = \left(\sum_{i=1}^{P} |\,\delta(i)\,|^2\right)^2 - \left|\sum_{i=1}^{P-1} \delta(i)\delta^*(i+1)\right|^2, \tag{7.13}$$

$$E_{P_{ACTD}}(\mathbf{X},\mathbf{Y}) = \left(\sum_{i=1}^{P} |\,\delta(i)\,|^2\right)^2, \tag{7.14}$$

where $\delta(i) = x(i) - y(i)$.

Using (7.12), (7.13) and (7.14) it can be easily shown that

$$E_{P_{ACTD}}(\mathbf{X},\mathbf{Y}) - E_{P_{DTD}}(\mathbf{X},\mathbf{Y}) = \left|\sum_{i=1}^{P-1} \delta(i)\delta^*(i+1)\right|^2 \geq 0\,, \tag{7.15}$$

and

$$E_{P_{ACTD}}(\mathbf{X},\mathbf{Y}) - E_{P_{OTD}}(\mathbf{X},\mathbf{Y}) = \left(\sum_{i=1}^{P/2} \mid \delta(2i-1) \mid^2 - \sum_{i=1}^{P/2} \mid \delta(2i) \mid^2\right)^2 \geq 2\,. \tag{7.16}$$

Therefore, for any pair of distinct information sequences, the product distance between their corresponding code matrices for the Alamouti scheme is always greater than or equal to the product distance between the code matrices associated with the other two schemes.

7.3 OUTER (CHANNEL) CODE DESIGN AND IMPLEMENTATION

The use of classical convolutional and turbo codes as the outer channel code in the STCM system is straightforward, and can readily be implemented as shown in Figure 7.1.

It is informative to note from (7.15) and (7.16) that on average for the inner codes, the ratios

$$\frac{E_{P_{ACTD}}(\mathbf{X},\mathbf{Y}) - E_{P_{OTD}}(\mathbf{X},\mathbf{Y})}{E_{P_{ACTD}}(\mathbf{X},\mathbf{Y})}\,, \tag{7.17}$$

and

$$\frac{E_{P_{ACTD}}(\mathbf{X},\mathbf{Y}) - E_{P_{DTD}}(\mathbf{X},\mathbf{Y})}{E_{P_{ACTD}}(\mathbf{X},\mathbf{Y})}, \tag{7.18}$$

decrease as P is increased. This observation indicates that the difference in performance between the Alamouti scheme and the other two schemes will be reduced by using more powerful outer channel codes having larger minimum Euclidean distances. With this objective in mind, the use of TCM and turbo TCM (TTCM) codes are proposed as outer channel codes in STCM transmit diversity.

The appropriate criterion for designing good TCM schemes for the AWGN channel is to maximize the minimum Euclidean Distance (ED) between any two distinct information sequences of the coded sequences. Several papers [234, 235] have shown that the error rate performance of TCM schemes over fading channels can be strongly influenced by the effective or shortest error event path, L_{min} and the minimum product distance, λ_L along that error event path. These parameters play a more important role than the minimum ED. For this reason MTCM codes have been designed in order to achieve superior performance on the fading channel, compared to that achievable by conventional TCM of the same throughput and decoder complexity.

A heuristic approach is adopted for the design of the outer TCM codes employing classical (MTCM) techniques. The advantage of the latter approach is that it provides a unified design procedure for these type of STCM systems, including the design of multi-level, multi-dimensional and asymmetric coded modulation schemes. In [203], Tarokh *et al.* proposed two design criteria, namely the rank and determinant criteria, for the design of STCM TDMA systems. Here, the two design criteria will be modified to be more closely related to the MTCM code construction process. Using this insight, the layered squared Euclidean distance (LSED) and layered squared Euclidean distance product (LSEDP) of the STCM system [236] are defined.

7.3.1 Code Design

In its most general form, MTCM is implemented by an encoder with b binary input bits and s binary output bits that are mapped into $\kappa\times$ QPSK symbols in each transmission interval. Figure 7.2 illustrates the proposed space-time MTCM encoder.

The parameter κ is referred to as the *multiplicity* of the code, since it represents the number of QPSK symbols allocated to each branch in the trellis diagram ($\kappa = 1$ corresponds to conventional TCM). To produce such a result, the s binary encoder output bits are partitioned into κ groups containing $m_1, m_2, \ldots, m_k$ symbols. Each of these groups, through a suitable mapping function, results in a QPSK output symbol.

Recall that with conventional trellis coding (i.e., one symbol per trellis branch), the length L_{min} of the shortest error event path is equal to the number of trellis branches along that path. A trellis diagram with parallel paths is constrained to have the shortest error event path of one branch, $L_{min} = 1$. This implies that the asymptotic region of the graph of average BEP will vary inverse linearly with $\overline{E_s}/N_o$ or E_s/N_o, since $\overline{E_s} = E_s$ [21]. Therefore, from an error probability viewpoint it is undesirable to design conventional TCM codes to have parallel paths in their trellis diagrams.

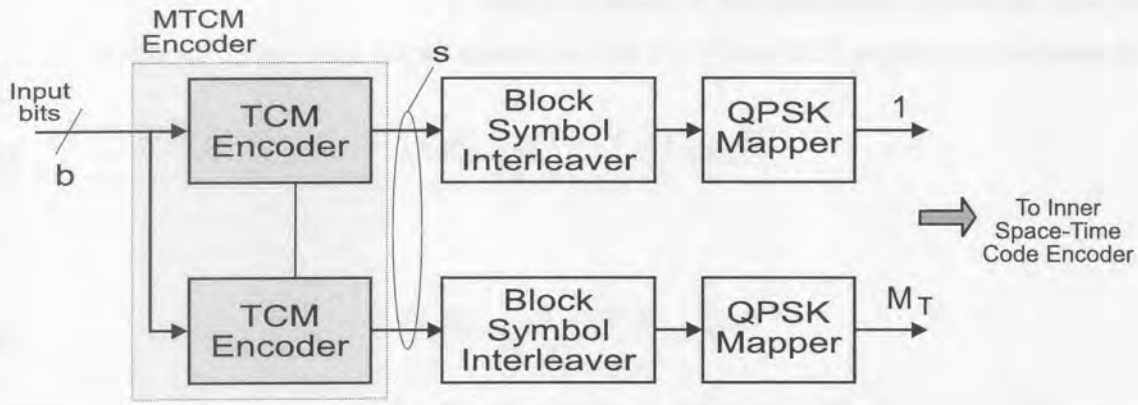

Figure 7.2. Space-time MTCM encoder and multiple transmit antenna diagram.

When the MTCM approach is employed for space-time code designs, the option of designing a trellis diagram with parallel paths may again be considered, since it offers more flexibility in selecting higher effective code lengths (or error event paths). The reason behind this lies in the fact that even if parallel paths exist in the trellis, it is now possible to have more than one coded symbol with non-zero ED associated with an error event path branch of length, $L_{min} = 1$.

In the design of the space-time codes a procedure similar to that presented in [21], known as the *Ungerboeck: From Root-to-Leaf* approach, has been followed. The set partitioning method, makes use of κ-fold Cartesian products of the sets found in Ungerboeck's original set-partitioning method for conventional trellis codes [24]. The set-partitioning procedure is started with a κ-fold Cartesian product of the complete QPSK signal set.

The latter multiplicity factor is the most important parameter in the space-time coding design procedure. In general, the design criteria do not include any direct considerations on the choice of multiplicity factor, κ, as a function of the channel parameters. In [237], it has been shown how the general design criteria for MTCM codes for fading channels, can be augmented by including an analysis of the lengths of burst errors. For the space-time transmission system under consideration the choice of κ is naturally determined by the number of available transmit antennas, n_T.

7.3.1.1 Ungerboeck Set Partitioning. Considering the code design for $M_T = 2$, the first step is to partition $A_0 \otimes A_0$ into M_c signal sets defined by the ordered Cartesian product $\{A_0 \otimes B_i\}$, $i = 0, 1, \ldots, M_c - 1$. The second element $\{j_2\}$ of B_i is defined by $nj + i \mod M_c$. In terms of the space-time mapping it is

appropriate to define a new design parameter, that will be called the LSED. Specifically, since the LSED between any pair of $\kappa = 2$-tuples is the sum of the distances between corresponding symbols in the 2-tuples, the set partitioning guarantees that the *intra-distance* (i.e., distance between pairs within a specific set or partition) of all of the partitions $A_0 \otimes B_i$ is identical. In addition, as a result of the possible existence of parallel paths in the decoding trellis, the minimum product of LSEDs must be maximized. This parameter is referred to as the LSEDP, is given by $\prod d_{ij}^2$.

Therefore, for the generating set $A_0 \otimes B_0$, the minimum LSEDP over all pairs of 2-tuples must be maximized. This is done by choosing the odd integer multiplier, n such that it produces the desired *maximin* solution. A computer search for possible values of n, revealed the solution to be $n = 1$. The sets, $A_0 \otimes B_i$, $i = 0, \ldots, M_c - 1$ for $M_T = \kappa = 2$, are illustrated below for QPSK.

$$A_0 \otimes B_0 = \begin{bmatrix} 0 & 0 & 1 & 1 \\ 2 & 2 & 3 & 3 \end{bmatrix}$$

$$A_0 \otimes B_1 = \begin{bmatrix} 0 & 1 & 1 & 2 \\ 2 & 3 & 3 & 0 \end{bmatrix}$$

$$A_0 \otimes B_2 = \begin{bmatrix} 0 & 2 & 1 & 3 \\ 2 & 0 & 3 & 1 \end{bmatrix}$$

$$A_0 \otimes B_3 = \begin{bmatrix} 0 & 3 & 1 & 0 \\ 2 & 1 & 3 & 2 \end{bmatrix}$$

Note that each set has a minimum intra-distance of $4E_b$. The *inter-distances* (i.e., minimum distances between pairs of 2-tuples from different sets), for these sets are summarized in Table 7.1.

Table 7.1. Inter-distances between partitioned subsets, with $A_0 \otimes B_0$ used as reference.

Subset	Distance	Subset	Distance
$A_0 \otimes B_0$	—	$A_0 \otimes B_1$	$4E_b$
$A_0 \otimes B_2$	$8E_b$	$A_0 \otimes B_3$	$4E_b$

Following tradition, the subsequent steps in the set-partitioning procedure are to partition each of the M sets $A_0 \otimes B_i$, into two sets $C_0 \otimes D_{i0}$ and $C_0 \otimes D_{i1}$, with the first containing the even elements ($j = 0, 2, \ldots, M_c - 2$) and the other containing the odd elements ($j = 1, 3, \ldots, M_c - 1$).

The sets, $C_0 \otimes D_{ij}$, using the procedure described in the foregoing are illustrated below.

$$C_0 \otimes D_{00} = C_0 \otimes D_{20} = \begin{bmatrix} 0 & 0 \\ 2 & 2 \end{bmatrix}$$

$$C_0 \otimes D_{01} = C_0 \otimes D_{21} = \begin{bmatrix} 1 & 1 \\ 3 & 3 \end{bmatrix}$$

$$C_0 \otimes D_{10} = C_0 \otimes D_{30} = \begin{bmatrix} 0 & 2 \\ 2 & 0 \end{bmatrix}$$

$$C_0 \otimes D_{11} = C_0 \otimes D_{31} = \begin{bmatrix} 1 & 3 \\ 3 & 1 \end{bmatrix}$$

Note that each set has a minimum intra-distance of $8E_b$ and the inter-distances for these sets are $8E_b$.

7.3.1.2 Outer Coder Implementation. The encoder and decoder configuration can be easily derived from the trellis diagram. The output channel signals are directly expressed in terms of a sliding block of input bits, with the intermediate step of output coded bits being irrelevant for analytically described trellis codes.

The realization of a rate-2/4 space-time trellis code of multiplicity $M_T = \kappa = 2$ is considered. Thus, two QPSK symbols are transmitted over the channel for every 2 bits accepted by the encoder. The input/output/state connection diagram for this coding system is shown in Figure 7.3 ((a) 2-state, (b) 4-state). It defines the sliding block of source variables $(b_1, b_2, b_3^{(1)}, b_4^{(1)}, b_3^{(2)}, b_4^{(2)})$. Note that the output bits $(b_3^{(z)}, b_4^{(z)})$, $z = 1, 2$ are mapped into the QPSK symbols output from the antenna elements.

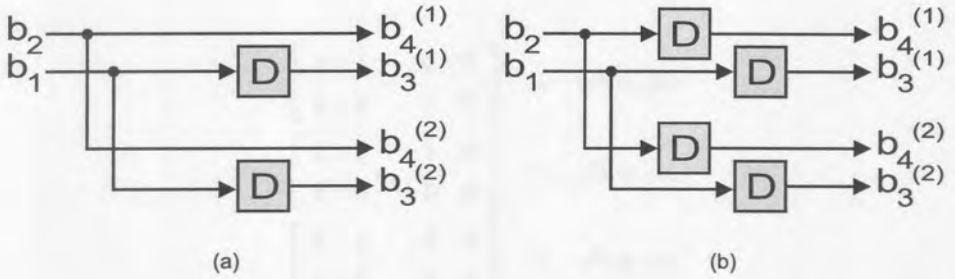

Figure 7.3. Space-time outer encoder input/output/state connection diagram (a) 2-state, (b) 4-state.

The code structure for the half-connected rate-2/4 space-time outer code is presented in Figure 7.4, for a cardinality of 2. The number of branches associated with each state (i.e., emanating from or terminating in a node) equals $2^2 = 4$.

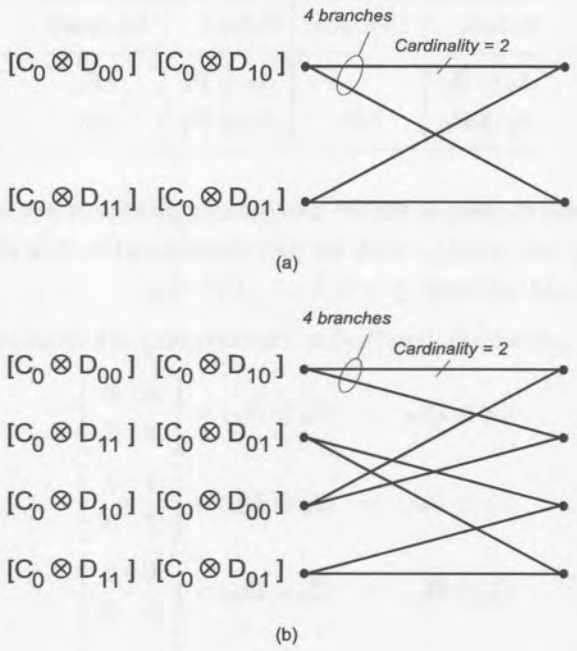

Figure 7.4. Trellis diagram of 4-state space-time code ($M_T = 2$) (a) 2-state, (b) 4-state.

7.3.2 *Extension to Space-time Turbo-Coded Modulation*

From the discussion in the previous section, it seems to be quite natural to combine bandwidth efficient MTCM with the ideas and concepts of space-time turbo codes. In [238, 239], Robertson has presented a straight forward approach of combining the two ideas of TCM and turbo codes into turbo TCM (TTCM for short). Here, the concepts of the latter are extended to turbo MTCM (T-MTCM) coded outer codes for the STCM transmit diversity scenario.

7.3.2.1 Turbo MTCM Encoder. Figure 7.5 shows the modified turbo MTCM (T-MTCM) encoder structure. The main difference between this encoder and the binary space-time turbo coding scheme is that the T-MTCM encoder operates on (multiple) symbols instead of bits.

The input of the encoder is now a block of N_{tc} information symbols with each symbol consisting of b information bits at a time. The information symbol sequence is directly processed by a rate-b/s MTCM encoder, and then by a second one after intermediate symbol-wise interleaving.

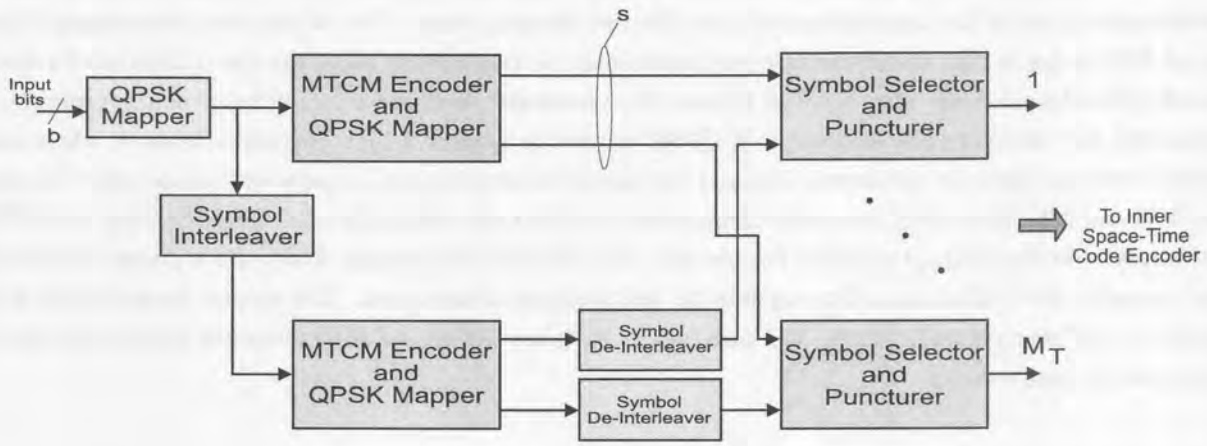

Figure 7.5. Space-time turbo MTCM encoder.

The MTCM encoders, forming the constituent turbo encoders, are designed as discussed in Section 7.3. Each encoder is immediately followed by a QPSK symbol mapper, that maps the code words onto the two-dimensional symbol plane. These output symbols of the two encoders are then alternately punctured to form the symbol streams to be transmitted at the different antennas.

From the figure it is noted that puncturing of the second encoder output takes place after previous de-interleaving, in order to restore the original order of the systematic part of the code symbols. This procedure ensures that each information symbol is only contained in one of the transmitted symbols, and the parity bit is alternately chosen from the first and second encoder. Thus, the complete code can be seen as systematic.

Interleaver (De-Interleaver) Structure. Interleaving should be performed similarly to the binary turbo coding scheme, with one exception: for T-MTCM, the input sequence is interleaved symbol-wise instead of bit-wise. All other characteristics remain the same, in particular the sub-interleaving according to the puncturing pattern of the two constituent encoder outputs as discussed earlier. The latter ensures, that the parity bits are uniformly distributed for each interleaver/de-interleaver combination.

QPSK Mapper. The mapper acts in exactly the same way as in conventional TCM schemes and assigns the non-binary code symbols to the set-partitioned phasors.

Puncturing. Normally puncturing is performed such that every second output symbol of the two constituent encoders is punctured alternately. In general any other code rates are achievable by applying different puncturing patterns to the encoder outputs.

7.3.2.2 Turbo MTCM Decoder. The iterative T-MTCM decoder is similar to the binary turbo decoder, except that there is a difference in the nature of the information passed from one decoder to another, and in the treatment of the first decoding step. This is due to the fact that – in contrast to the binary case – the systematic information is transmitted together with the parity information in the same modulation symbol. Therefore, the systematic component cannot be separated from the extrinsic one. And again, the decoder now processes symbols instead of bits.

In the binary turbo coding scheme, the constituent decoders' output is split into three additive parts for each information bit: the intrinsic or systematic component that corresponds to the received systematic value for the bit concerned, the *a priori* component that is the information given by the other decoder for the bit, and the extrinsic component that is derived by the decoder itself, depending on all the other inputs. Only the extrinsic component may be passed to the next decoder, that uses it as the *a priori* component, in order to avoid multiple use of the same information in different decoding steps. One of the great advantages of the use of RSC codes is that the systematic part needs only be transmitted once, since it is identical for both encoder/decoder combinations. If BPSK is used, the systematic and the parity information are transmitted separately and therefore are separable. If QPSK is used to achieve a high spectral efficiency, where one symbol contains both the systematic bits and the parity information, this separation is impossible because the MAI and noise that affect the parity component also affect the systematic one. Therefore, the T-MTCM component decoders' output can only be split into two different components: firstly the *a priori* component and secondly the combination of the systematic and extrinsic components. The second component is now passed to the next decoding stage, and care has to be taken not to use the systematic information more than once in each decoder.

7.3.3 Outer Code Performance

Thus far the BEP performance discussion has focused on the performance gain as measured by the improvement in minimum free Euclidean distance of the inner trellis code. Using superstate diagrams and upper bounds on the BEP performance computed from the transfer functions of these diagrams, the outer coder performance gains are evaluated.

Analogous to the analytical techniques discussed in Chapter 4, an upper bound on the BEP performance of MTCM is given by [21, 234, 235, 240]

$$P_e \leq \frac{1}{b} Q\left(\sqrt{\frac{bE_b}{\kappa N_0}\frac{d_{free}^2}{4}}\right) Z^{-d_{free}^2} \frac{\delta}{\delta I} T(I,D)\,|_{I=1,D=Z}\,, \tag{7.19}$$

where Z is the Bhttacharyya parameter defined by

$$Z = \exp\left(-\frac{1}{4}\frac{E_s}{N_0}\right) = \exp\left(-\frac{1}{4}\frac{bE_b}{\kappa N_0}\right)\,, \tag{7.20}$$

with E_s the energy per trellis code symbol, and $T(I,D)$ the transfer function of the superstate diagram associated with the multiple trellis code.

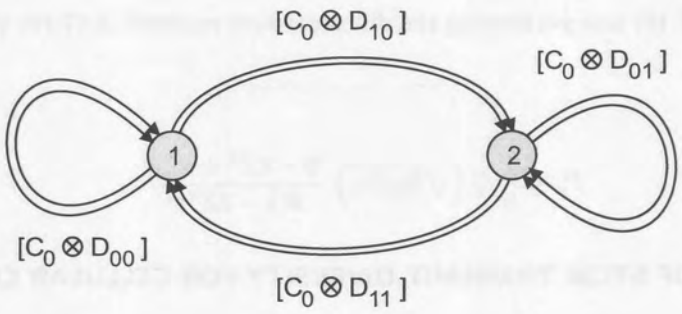

(a)

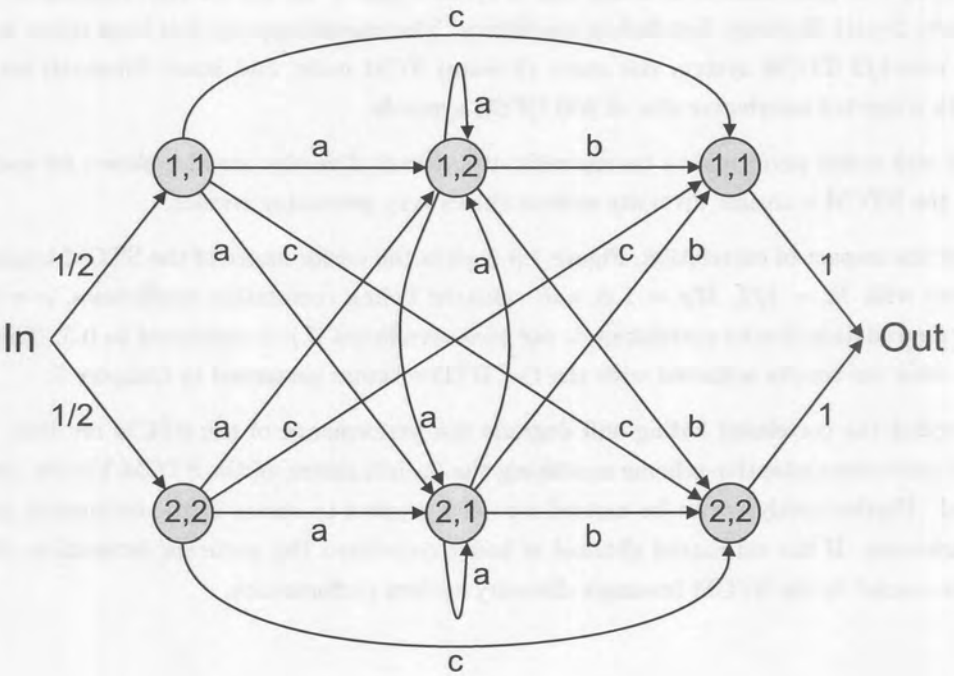

(b)

Figure 7.6. (a) State and, (b) Superstate diagram for rate-$2/4$ space-time outer code.

The performance of the 2-state rate-2/4 TCM inner code with trellis diagram as in Figure 7.4(a) is considered. The corresponding state diagram is illustrated 7.6(a), and the equivalent superstate diagram for computing $T(I, D)$ is shown in Figure 7.6(b). The branch labels are

$$a = \frac{1}{2}(I + I^2)\, D^4, \quad b = \frac{1}{2}(1 + I)\, D^4, \quad c = \frac{1}{2} I\, D^4 \,. \tag{7.21}$$

From Figure 7.6(b), in the absence of fading, the transfer function is easily computed as

$$\begin{aligned} T(I, D) &= 2c + \frac{4ab}{1 - 2a} \\ &= \frac{(2I + 2I^2 + I^3)\, D^8 - I^2 + I^3)\, D^{12}}{1 - (I + I^2)\, D^4} \,. \end{aligned} \tag{7.22}$$

Substituting (7.21) into (7.19) and performing the differentiation required in (7.19) yields the desired upper bound on the BEP

$$P_e \leq \frac{1}{8} Q\left(\sqrt{E_b/N_0}\right) \frac{9 - 8Z^4 + 4Z^8}{9(1-2Z^4)^2} . \tag{7.23}$$

7.4 PERFORMANCE OF STCM TRANSMIT DIVERSITY FOR CELLULAR CDMA

Making use of (7.23), (3.29), (4.6), the approximated BEP performance of a cellular CDMA system employing space-time trellis coded transmit diversity can be determined numerically.

Figure 7.7 depicts the performance as a function of system load, V for the STCM transmit diversity system operating under 2-path Rayleigh fast-fading conditions. The operating point has been taken as $E_b/N_0 = 20$ dB. For the rate-1/2 STCM system the outer (2-state) TCM code, and inner Alamouti code have been assumed, with a symbol interleaver size of 200 QPSK symbols.

The uncoded and coded performance curves without transmit diversity are also shown for comparison. As can be seen, the STCM transmit diversity system shows very promising results.

To investigate the impact of correlation, Figure 7.8 depicts the performance of the STCM transmit diversity CDMA system with $R_c = 1/2$, $M_T = 1, 3$, and constant fading correlation coefficients, $\rho = 0.0, 0.5$. The performance degradation due to correlation is not that significant if ρ is restricted to 0.5. This observation is consistent with the results achieved with the O-CDTD schemes presented in Chapter 5.

If left unattended the correlated fading will degrade the performance of the STCM receiver. Under these conditions, a space-time adaptive scheme modifying the branch metric of the STCM Viterbi decoder should be considered. Further analysis can be carried out with respect to errors in the estimation process of the channel parameters. If the estimated channel is badly correlated the accurate estimation of the channel parameters is crucial to the STCM transmit diversity system performance.

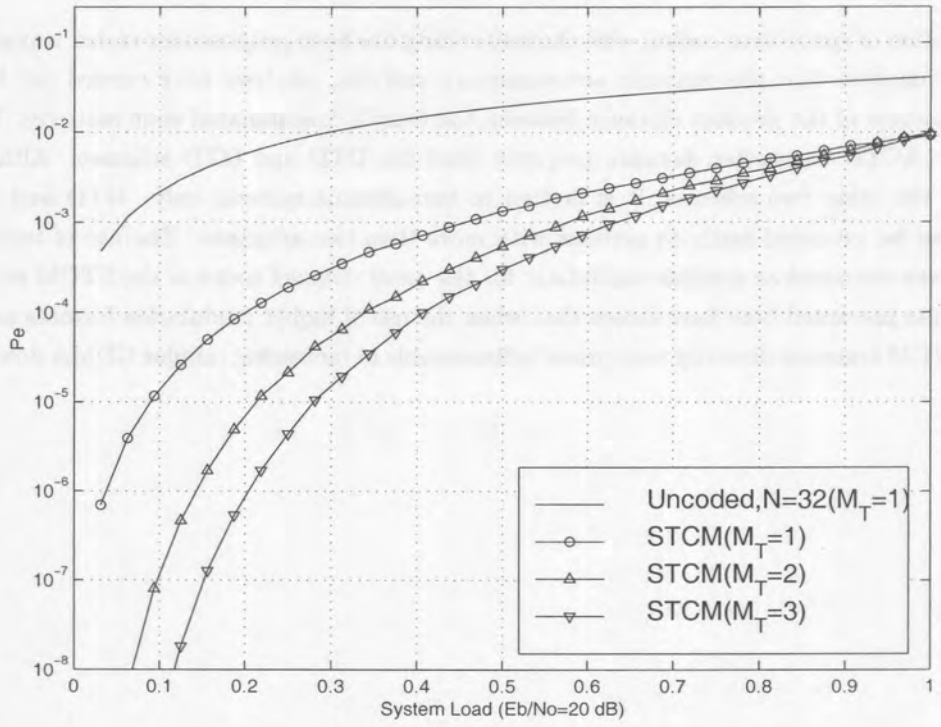

Figure 7.7. STCM transmit diversity performance on a 2-path fading channel with $R_c = 1/2$ and $M_T = 1, 2, 3$.

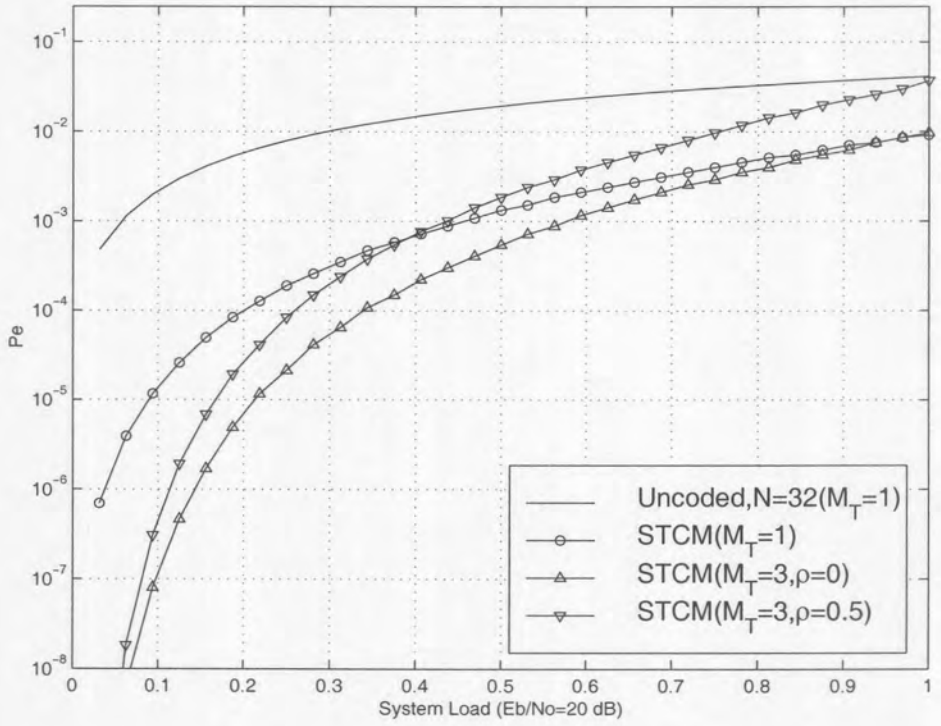

Figure 7.8. STCM transmit diversity performance on a correlated 2-path fading channel with $R_c = 1/2$ and $M_T = 1, 3$.

7.5 SUMMARY

The concatenation of space-time coding with channel coding has been proposed for coded transmit diversity. Under the assumption that the channels are stationary and flat, analysis were carried out based on the pairwise comparison of the product distance between the overall concatenated code matrices. It was shown that the inner ACTD has better distance property than the DTD and OTD schemes. Although ACTD is superior to the other two schemes, it is limited to two-antenna systems only. OTD and DTD on the other hand, can be extended easily to systems with more than two antennas. The use of trellis and turbo trellis codes were discussed as possible candidates for the outer channel coder in the STCM strategies. The analytical results presented here have shown that when the use of higher modulation formats are considered for CDMA, STCM transmit diversity may prove indispensable in increasing cellular CDMA downlink system capacity.

8 CODED SPACE-TIME RECEIVE DIVERSITY AND BEAMFORMING

In the previous three chapters the performance of space-time coded multiple transmit antenna diversity systems have been evaluated for improving the downlink capacity. In this chapter coded space-time processing for the uplink, namely receive diversity and beamforming, are discussed.

Recall, any mapping of information carrying symbol (or bit) sequences into a spatial-temporal code matrix is referred to as a space-time code. Following this convention, it should be clear that the coding techniques to be used with multiple receive antenna cannot be regarded as "true" space-time coding. For this reason these are referred to as coded space-time processing since the type of space-time receiver will influence the choice of FEC coder.

This chapter uses the system model and analysis presented in Chapter 3 in conjunction with the space-time channel model presented in Chapter 2 and the coding bounds derived in Chapter 4 to evaluate the performance of the space-time CDMA systems. Specifically, the performance of a convolutional and turbo coded CDMA system in a receive diversity environment, and a beamforming environment is considered.

8.1 CODED SPACE-TIME RECEIVE DIVERSITY PERFORMANCE

Making use of (3.23), (3.28), (3.29) and (4.6) the BEP performance of a CDMA system using coded space-time receive diversity are considered here, The assumed system parameters as outlined in Table 8.1.

Figure 8.1 depicts the BEP performance of MRC receive diversity CDMA under 2-path Rayleigh fast fading conditions, with rate $R_c = 1/2$ convolutional and turbo ($N_{tc} = 256, 2048$) coding. The number of users are taken as $K = 5$ with $M_T = 1, 2$ and 3 receive antenna elements.

Figures 8.2 and 8.3 depict the performance as a function of system load, V for coded CDMA employing MRC receive diversity. The operating point has been taken as $E_b/N_0 = 20$ dB.

By introducing multiple receive antennas, the diversity order is increased, resulting in a improvement in the composite fading signal. Thus, the probability of coding gain is increased. From the graphs it clear that turbo coded transmit diversity increases the performance substantially.

Parameter	Simulation value
Spreading sequence length	$N = 32$
Operating environment	2-Path, equal strength.
User distribution	uniform
Number of multi-path signals	$L_p = 2$
Number of users	$K = 1, 2, \ldots, N$
Number of RAKE fingers	$L_R = 2$
Transmit diversity elements	$M_T = 1$
Receive diversity elements	$M_R = 1, 2, 3\ \rho = 0, 0.5$

Table 8.1. System parameters for numerical evaluation of coded receive diversity CDMA BEP performance.

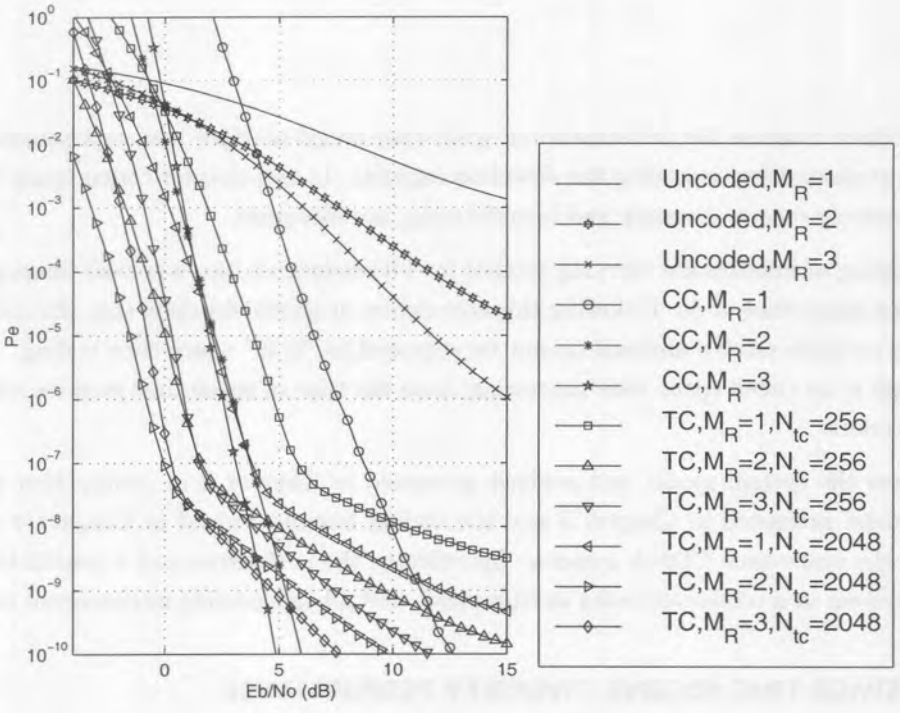

Figure 8.1. Analytical BEP performance of coded MRC receive diversity, with $R_c = 1/2$, $K = 5$, and $M_R = 1, 2, 3$, on a fast fading 2-path channel.

With reference to Figure 8.3, it is clear that the correlation between the M_R diversity elements influences the achievable BEP performance. Thus, when designing the diversity system, the assumption that the signals received at each element are uncorrelated cannot be used in BEP computations. Specifically, the presence of correlation between the fading envelopes of signals received at the various diversity branches will increase the BEP.

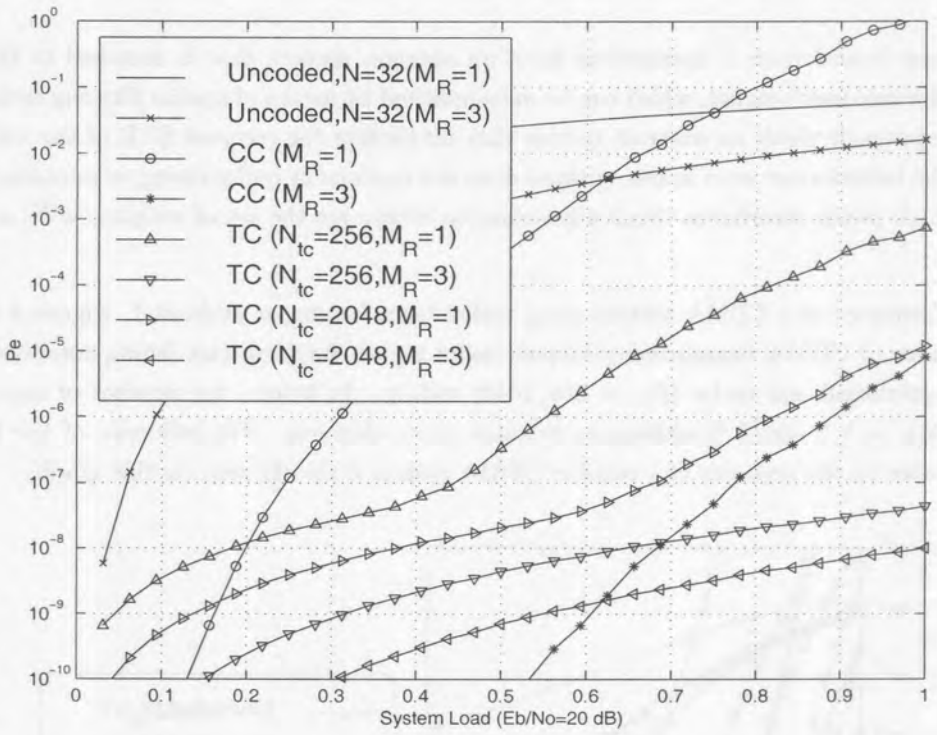

Figure 8.2. Coded O-CDTD performance comparison with $R_c = 1/2$, $N_{tc} = 256, 2048$ and $M_R = 1, 3$.

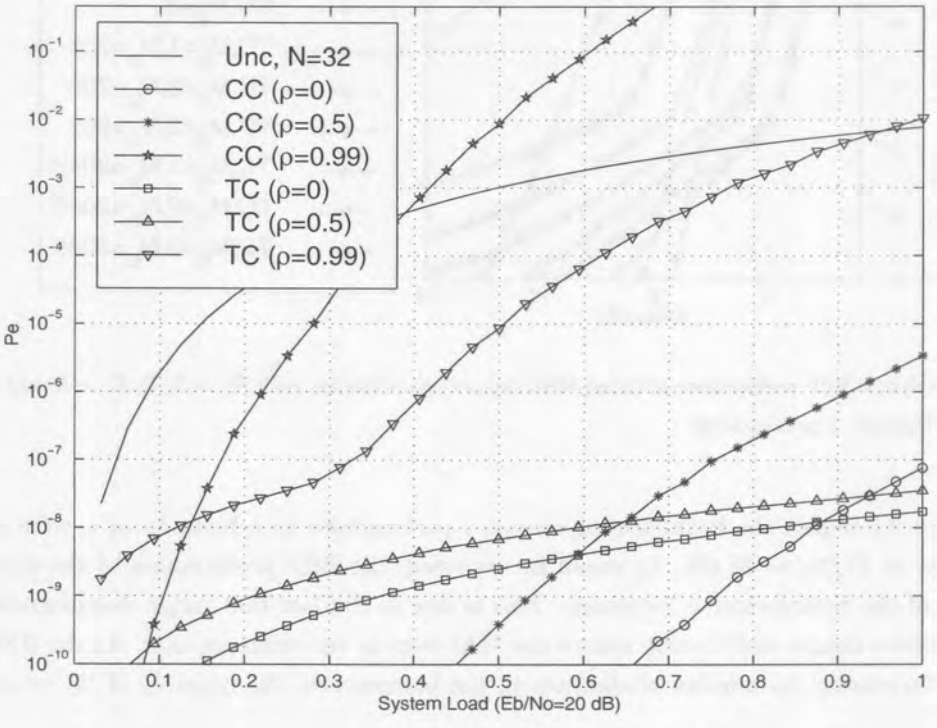

Figure 8.3. Comparison of $R_c = 1/2$ convolutional and turbo coding ($N_{tc} = 256, 2048$), with $M_R = 3$ and $\rho = 0, 0.5, 0.99$.

8.2 CODED SPACE-TIME BEAMFORMING ARRAY PERFORMANCE

The M_B element beamformer is assumed to form an antenna pattern that is matched to the pdf of the DOA of the reference user's signal, which can be accomplished by means of spatial filtering techniques. This beamforming approach yields an antenna system that maximizes the received SNR of the reference user's signal. Also, the beamformer used in this analysis does not implement null-steering to minimize interference from specific high power interferers. Such algorithms to determine the set of weights, $\mathbf{w}^{(k)}$, are treated in [126].

The BEP performance of a CDMA system using coded beamforming is evaluated. Figure 8.4 depicts the BEP performance of CDMA beamforming system under 2-path Rayleigh fast fading conditions, with rate $R_c = 1/2$ convolutional and turbo ($N_{tc} = 256, 2048$) coding. As before, the number of users is taken as $K = 5$ with $M_B = 1, 2$ and 3 beamforming antenna array elements. The influence of the beamforming antenna array size on the capacity of a cellular CDMA system is clearly seen on this graph.

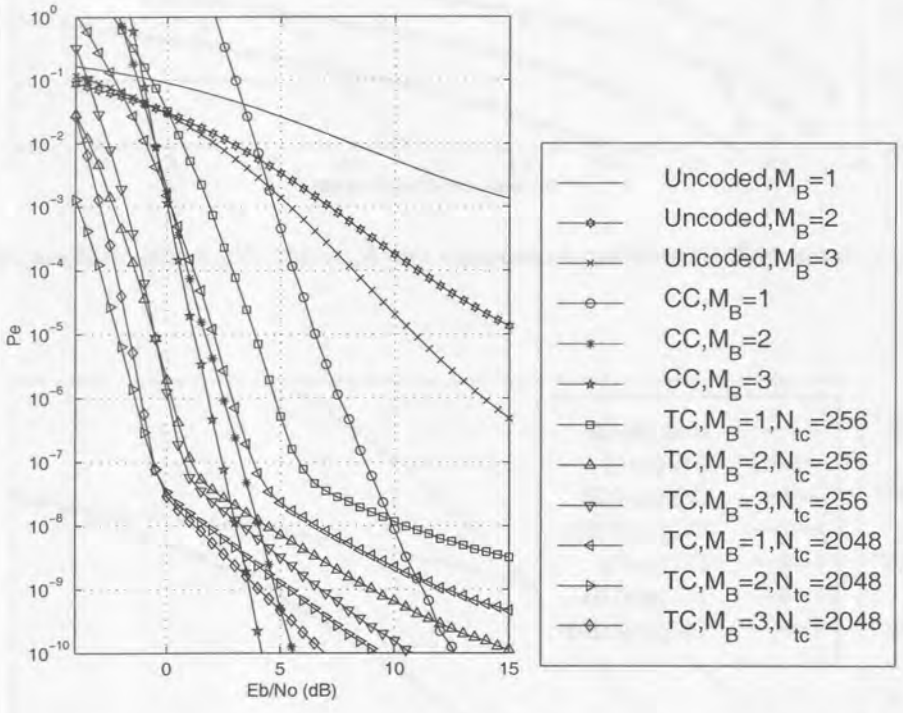

Figure 8.4. Analytical BEP performance of coded MRC receive beamforming, with $R_c = 1/2$, $K = 5$, and $M_B = 1, 2, 3$, on a fast fading Rayleigh 2-path channel.

Figures 8.5 and 8.6 depict the beamforming system's performance as a function of system load, V, at a operating point of $E_b/N_0 = 20$ dB. As would be expected, the BEP performance of the system is better when the size of the beamformer is increased. This is due to the fact that larger beamforming arrays can synthesize narrower beams and thereby reduce the MAI seen by the reference user. As the BEP probability is reduced by increasing the number of elements in the beamformer, the capacity of the cellular system is also increased.

Comparing the BEP performance of the beamforming (Figures 8.5 and 8.5) system with that of the receive diversity system (Figures 8.2 and 8.2), it can be seen that the beamformer BEP results are significantly better. As would be expected, the absolute BEP performance is worse as a result of the fading that is

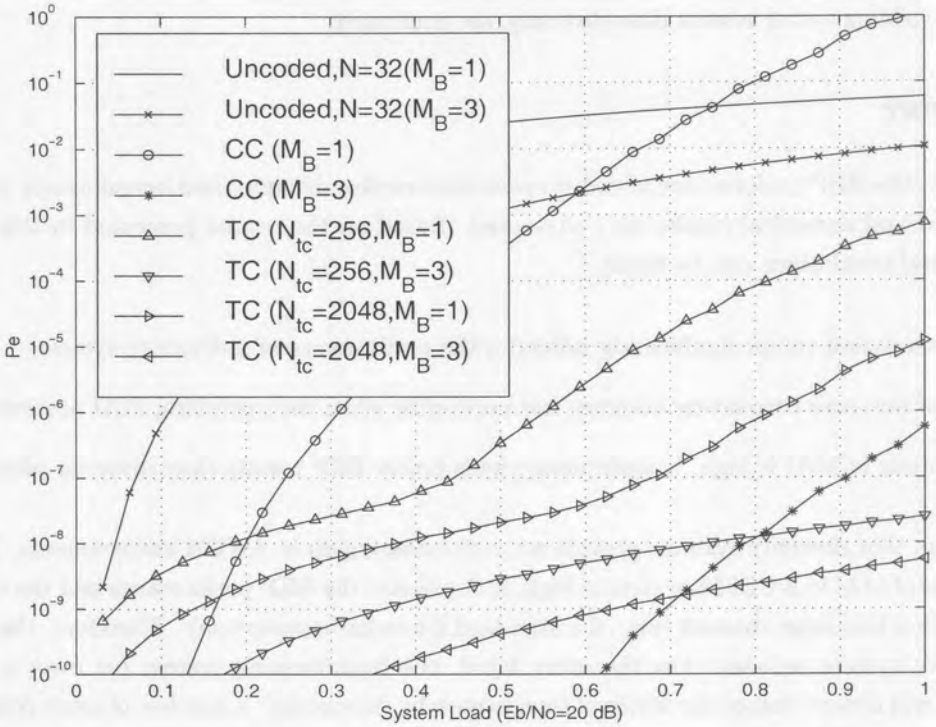

Figure 8.5. Coded MRC receive diversity performance comparison with $R_c = 1/2$, $N_{tc} = 256, 2048$ and $M_B = 1, 3$.

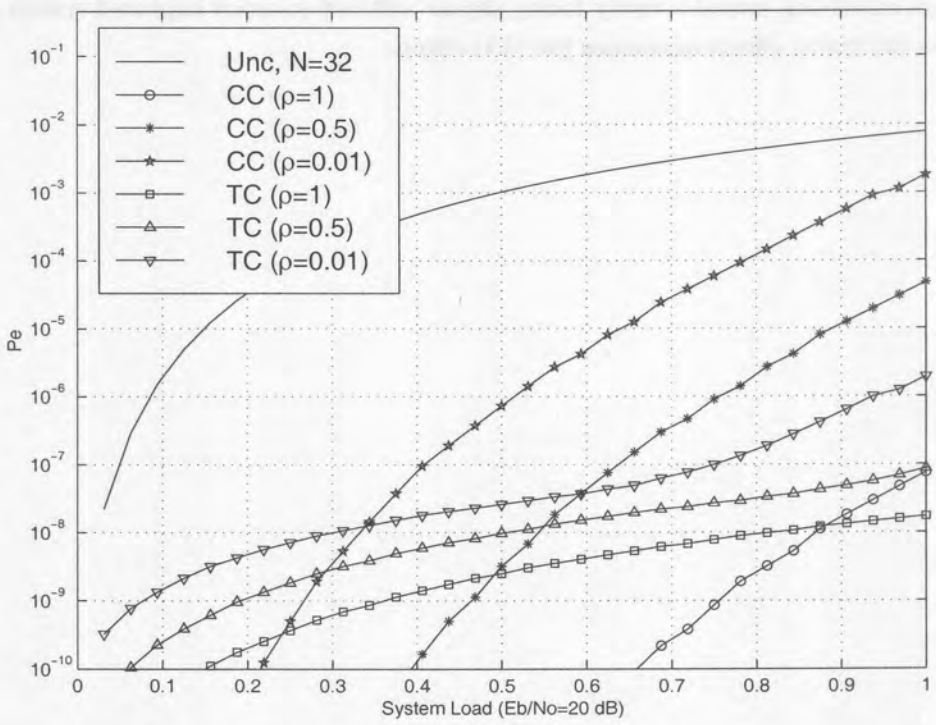

Figure 8.6. Comparison of $R_c = 1/2$ convolutional and turbo coding ($N_{tc} = 256, 2048$), with $M_B = 3$ and $\rho = 0, 0.5, 0.99$.

more severe, however, the general trends of correlation negatively influencing diversity performance and beamforming yielding better results than diversity, are continued.

8.3 SUMMARY

In this chapter, the BEP performance of coded space-time receive diversity and beamforming processors has been addressed and numerical results were presented. Based on the results presented in this chapter, the following general conclusions can be made

- Non-zero correlation values significantly influence the performance of a diversity system.
- The effect of non-zero correlation becomes less noticeable when the prevailing MAI present is high.
- When the levels of MAI is high, beamforming yields better BEP results than diversity alone.

It is well known that diversity systems provide no performance gain in AWGN environments. Furthermore, when the levels of MAI in a CDMA system is high, it dominates the BEP performance and the channel starts to approximate a Gaussian channel (viz. the standard Gaussian assumption). Therefore, the effectiveness of the diversity system reduces. On the other hand, the beamforming system (or even a system with sectorization) will always reduce the levels of interference by "removing" a number of users from the system resulting in better BEP performance. The contrary is also true. When the number of users are low, and the channel is severely fading (as in the NLOS case), the beamforming system cannot improve the receive signal as it does not add any new information to the received signal, but merely limits the MAI. Thus, beamforming systems do not achieve high performance gains. In severe fading, on the other hand, a diversity system combining several severely fading signals will lead to much improved system performance, especially when the fading effects dominates the MAI effects.

9 SUMMARY AND CONCLUSIONS

In this final chapter, a summary of the most important results and conclusions of this thesis is given. The goals of the thesis as outlined in the introductory chapter are revisited and it is stated whether the goals have been reached. In addition future areas of research yet to be explored are also highlighted.

9.1 GOALS OF THE THESIS

The main focus of the research has been on coded space-time processing techniques, which were presented in the context of designing mobile communication systems where the two core areas of spatial processing and error coding have to be integrated in an optimum way. The main goals of the thesis are given below and it is shown whether these have been met.

- To establish a general spatial/temporal channel model for use in the evaluation of coded space-time processing concepts applied to CDMA networks.
  - A spatial/temporal channel model for the evaluation of cellular systems incorporating smart antenna techniques has been developed (see Chapter 2). Amongst the many parameters incorporated in this model, the ability to model the influence of local scatters on the fading envelope correlation has been shown to be of utmost importance in the performance evaluation of space-time coded systems.
- To analyze the performance of uncoded cellular CDMA systems incorporating space-time techniques using analytical methods under a number of realistic application scenarios.
  - BEP performance has been determined in integral form, where the integral is easily evaluated using numeric integration techniques, based on the above mentioned channel model.
- To design, implement and evaluate coding strategies for incorporation into the space-time CDMA systems. This objective has been broken down into
  - Space-time coding systems when considering multiple transmit antennas for the downlink.

    - * Layered space-time convolutional and turbo coded transmit diversity systems have been considered. The techniques included CDTD and TDTD.
    - * Novel extensions to layered space-time configurations, viz. PSTTD, SCTTD and SOTTD, have been proposed.
    - * The application of trellis codes and turbo trellis codes have been considered in Chapter 7.
  - Coded space-time systems when considering multiple receive antennas for the uplink.
    - * Classical convolutional and turbo coded space-time receive diversity and beamforming have been considered.

- To establish the performance of coded space-time CDMA cellular networks under realistic scenarios.
- Underpinned by a comprehensive chapter on the derivation of FEC coding upper bounds, the BEP performances of all the above mentioned space-time coding techniques have been carried out.

9.2 SUMMARY

In order to establish a frame of reference for the evaluation of the contribution of this work, a brief overview of some emerging wireless technology application has been given in Section 1.1. In this overview, it has been shown that many new wireless access solutions, such as UMTS, will incorporate space-time techniques as one method of increasing overall system capacity. A literature survey of forward error correcting codes and space-time processing techniques has been presented as basis for the work covered in this thesis.

In Chapters 2 to 3, extensive background information on channel impairments and space-time channel and system models have been presented. It has been shown that path loss, fading, scattering environment and user distribution are some of the key aspects limiting the performance of space-time processing systems and is crucial in determining mitigation techniques. Together, these chapters provided the necessary background information required to understand the specifics of the two main space-time techniques covered, namely adaptive beamforming, and transmit/receive diversity. The BEP performance of these space-time processors has been derived analytically and numerical results were presented. Based on the analytic results, the effects of the number of antenna elements and correlation between branches on BEP performance of the space-time processing techniques have been addressed. The BEP sensitivity of all the space-time techniques to fading correlation (or lack of it for the beamforming case) were illustrated.

Chapter 4 presented a detailed discussion of the channel coding techniques, including classical convolutional and turbo, and trellis codes for cellular CDMA systems. The BEP performance of these codes has been addressed by the derivation of analytical average upper bounds based on the union bound and code weight distributions. Numerical results were presented.

In Chapter 5 space-time coded transmit diversity techniques have been introduced as a means to improve cellular CDMA performance. The suitability of convolutional- and turbo coding, when applied to layered space-time transmit diversity, has been discussed and analytical results presented for CDTD and TDTD under conditions of multipath fading. The analytical results have shown that the combining of spatial and temporal processing at the transmitter provides an effective way to increase CDMA system capacity in the downlink. In Chapter 6 extensions of CDTD have been presented in the form of TTD, including PCTTD, SCTTD and SOTTD. These schemes have the ability to improve the cellular capacity even further.

In Chapter 7 the concatenation of space-time coding with channel coding has been proposed for coded transmit diversity. The novel use of trellis and turbo trellis codes have been discussed as possible candidates

for the outer channel coder in the STCM strategies. It was shown that the inner ACTD has better distance property than the DTD and OTD schemes.

As a means of improving cellular CDMA uplink system performance and capacity, Chapter 8 has presented the BEP performance of coded space-time receive diversity and beamforming processors. Numerical results were presented and basic guidelines for choosing between diversity, beamforming and combined diversity and beamforming systems have been discussed.

9.3 AREAS FOR FUTURE RESEARCH

This research has highlighted a number of avenues yet to be explored. These avenues fall into two broad categories, namely further parametric and performance investigations of the existing transmit diversity schemes, and the investigation of new space-time coding structures for CDMA.

Parametric and Performance Investigation. Many space-time transmit diversity schemes have been introduced in this thesis. For all of these schemes only the most general descriptions were given, and limited performance evaluations were carried out. In this regard many parametric and performance investigations can and should still be performed. This is necessary to form a complete picture of all the issues involved and performance gains over a wide range of operating conditions.

Some ideas of these future investigations are listed below:

Performance investigations. In the performance analysis carried out in this thesis perfect power control has been assumed. By perfect power control it is implied that all signals received at the base station (or mobile terminal) are of equal power. Fortunately, when considering the performance of the downlink, the assumption of perfect power control is not necessarily bad, since the near-far problem is more common to the uplink. In practice, when the number of users is large and the power control is not perfect, the performance loss can be substantial. For this reason, future work should address the situation of non perfect power control on the space-time systems for both the uplink and downlink.

Parametric investigations. In the practical implementations of space-time transmit/receive and beamforming systems, many configurations and parameter selections may be considered. In order to form a complete assessment of the advantages on offer by the different space-time coded schemes the crossover point between complexity and performance improvement should be determined. For instance, it is possible to improve the performance of all the turbo coded systems simply by choosing a different interleaver, or by employing a different decoding configuration. Also, the performance of these schemes will vary significantly according to the size of the interleaver, and comparisons between the different schemes should be performed as a function of decoding complexity and desired transmission delay.

New space-time coding structures. The conventional matched filter receiver is optimal in a single user scenario with only AWGN. In a multiuser CDMA system with MAI, the performance is degraded and its only acceptable with accurate power control, error correction coding and relatively low load. It fails terribly in a near-far situation or if the number of simultaneous users is large. One way to improve the performance of cellular CDMA systems is to use interference cancellation and multiuser detection techniques to exploit the structure of the MAI and jointly detect (and decode) the users. It is important to note that multiuser detection does not necessarily mean that the system ceases to be interference limited but it improves the performance and removes the immense sensitivity to MAI.

There are two possible approaches to the use of space-time coding and multiuser detection in a receiver:

- The multiuser detection algorithm is applied first, and the soft/hard outputs are processed by the space-time decoding algorithm.
- The space-time decoding is performed if possible within the multiuser detection algorithm, so that the data estimates that are used to estimate the MAI components are those which have been error-corrected and are thus more reliable.

In [26], the optimal ML receiver for joint decoding is proposed. As both the CDMA channel and the FEC encoders are described by finite state machines, they each impose a trellis structure on the transmission. The joint effect can be described by a joint finite state machine with a corresponding super trellis. A linear approach is taken in [241] to accommodate joint detection and decoding based on the decorrelator. This decoder is based on incorporating the linear decorrelating process into the FEC decoder by modifying the metric. In effect, the projection receiver in [241] is a decorrelating detector followed by an FEC detector based on the Mahalanobis distance [242] rather than the Euclidean distance normally used. In [243] FEC decoding is incorporated into an interference structure. By embedding Viterbi decoding within the cancellation structure, significant improvements are achieved at the expense of a substantially increased detection delay. Even further improvements can be achieved by letting the bandwidth expansion be done entirely through low-rate error control coding.

With the current developments in digital signal processing technology these techniques may be considered for inclusion into the mobile handset. As a matter of fact, the present WCDMA proposal supports interference cancellation at the mobile terminals. Therefore, future research should be focused on the combination of multiuser detection and space-time coding processing. Along these lines turbo processing may again be considered, with the combined strategy of iterative feedback decoding, diversity combining and multiuser detection.

9.4 CONCLUSION

This thesis has introduced many (some novel) space-time turbo coded techniques to increase the downlink capacity of a cellular CDMA network using multiple transmit antennas. For improving the uplink capacity, coded space-time diversity and beamforming techniques, employing multiple receive antennas, have been considered. In order to quantify the performance improvements that may be achieved, a framework for the evaluation of these systems has been constructed. Using this framework the BEP of all the space-time coding systems have been derived analytically, and evaluated under identical propagation scenarios.

The results of this thesis have shown that the use of space-time turbo coded processing is an attractive solution since it can improve system performance significantly under conditions of multipath fading for both the uplink and downlink. It was shown that the two core areas of spatial processing and channel coding can be integrated in an optimum way to increase the capacity of existing cellular CDMA networks. It is envisioned that designers of future CDMA systems and networks will work towards the goal of the optimal combination of the processing involved with iterative (turbo) decoding, diversity signalling and multiuser detection. In line with this vision, the work presented in this thesis may be used as basis for the design and evaluation of these future multiuser space-time cellular CDMA networks.